

## Characterization and Crystal Structure of a Chiral Ruffled Basket-Handle Porphyrin

Philippe Richard, Eric Rose,<sup>†</sup> and Bernard Boitrel\*

Laboratoire de Synthèse et d'Electrosynthèse  
Organométalliques, "LSEO" (UMR CNRS 5632),  
6 Boulevard Gabriel, 21000 Dijon, France

Received May 4, 1998

### Introduction

For several decades, understanding the role of proteins such as myoglobin or hemoglobin in regulating and discriminating the binding of small molecules has been a topic of active interest. Particularly, one begins to understand how the affinity of an iron(II) porphyrin for the binding of carbon monoxide can be lowered versus the binding of dioxygen. Indeed, unhindered model hemes in organic solvents bind dioxygen and carbon monoxide with a ratio that favors CO over O<sub>2</sub> by an average factor of 65 000.<sup>1</sup> When the heme is embedded in a protein such as myoglobin, the ratio decreases to about 85. The close proximity of HisE7 to the ligand binding site led to the proposal that this residue serves to hinder sterically the binding of CO and thus reduces its affinity for myoglobin and hemoglobin.<sup>2</sup> Several models have been synthesized to probe this hypothesis, and different explanations have been advanced<sup>3</sup> to explain this spectacular property although only a limited number of crystal structures of the CO adduct are available.<sup>3a,4</sup> Some years ago, we reported the lowest value (105) described at that date<sup>5</sup> for

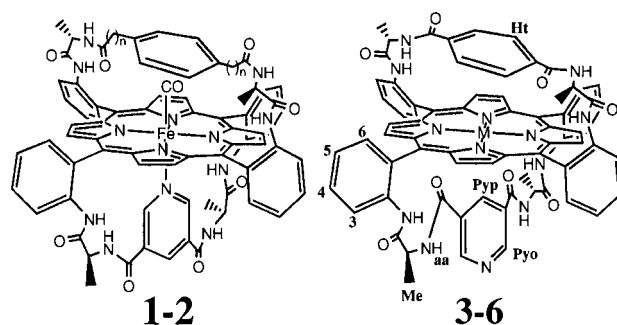


**Figure 1.** Chemical structures of the different models: **1**,  $n = 1$ , ArC<sub>2</sub>-PyFeCO; **2**,  $n = 0$ , ArPyFeCO; **3**, M = 2H, ArPyH<sub>2</sub>; **4**, M = Fe, ArPyFe; **5**, M = Zn, ArPyZn; **6**, M = Ni, ArPyNi.

M = K(CO)/K(O<sub>2</sub>) with porphyrin ArC<sub>2</sub>PyFeCO (**1**) bearing a homoterephthalic handle (Figure 1). We proposed that the Fe–CO bond of the porphyrin ArPyFeCO (**2**) with a simple terephthalic handle should have a different geometry with respect to the porphyrin plane than the expected linear geometry of the less sterically demanding porphyrin ArC<sub>2</sub>PyFeCO (**1**). We also suspected a nonlinear Fe–CO bond for ArPyFeCO (**2**) if the porphyrin plane is flat or a linear Fe–CO bond if the porphyrin plane is distorted. This conclusion could be reached on the basis of NMR spectroscopy results.<sup>6</sup> Despite extensive efforts, single crystals suitable for crystallographic studies of either **4** or **2** have not been successfully obtained to date. That is the reason we report herein the crystal structure of the porphyrin derivative ArPyNi (**6**), which is the nickel(II) counterpart of **4**.

### Experimental Section

**Chemicals.** All chemicals were of reagent grade quality. Merck TLC-Kieselgel (60H, 15 μm) silica gel was used for column flash chromatography.

**Instrumentation.** <sup>1</sup>H NMR spectra were recorded on a Bruker DRX 500 spectrometer and referenced to the residual proton solvents. UV–visible spectra were recorded on a Varian Cary 1 spectrophotometer. Elemental analyses were obtained on an EA 1108 Fisons Instruments apparatus.

**Synthesis of ArPyH<sub>2</sub> (3).** The free-base porphyrin was obtained by condensation of *N*-Boc-(S) alanine on the atropisomer αβαβ of tetra-*o*-aminophenylporphyrin (TAPP), deprotection of the amino group, and condensation of two different diacyl chlorides in high dilution conditions as described in the literature.<sup>7</sup>

**Synthesis of ArPyNi (6).** In a typical reaction, a solution of ArPyH<sub>2</sub> (**3**) (120 mg, 0.094 mmol) in CHCl<sub>3</sub> was mixed with a saturated solution of nickel bromide in methanol (20 mL) and heated to 50 °C overnight. After filtration, the solution was then evaporated to dryness, dissolved in dichloromethane, poured on a flash chromatographic column and eluted with 4% MeOH/CH<sub>2</sub>Cl<sub>2</sub> (yield 78%). Crystals suitable for X-ray were then obtained by evaporation of a solution of the porphyrin complex in CHCl<sub>3</sub>/MeOH/*n*C<sub>6</sub>H<sub>14</sub> over a 3-month period. Anal. Calcd for C<sub>71</sub>H<sub>55</sub>N<sub>13</sub>NiO<sub>8</sub>·8H<sub>2</sub>O: C, 60.01; H, 5.04; N, 12.81. Found: C, 59.93; H, 5.23; N, 12.18. UV–vis (CHCl<sub>3</sub>): λ nm (10<sup>-3</sup> ε M<sup>-1</sup> cm<sup>-1</sup>) 415 (277); 527 (45); 564 (31). <sup>1</sup>H NMR (500 MHz, CDCl<sub>3</sub>): 8.65 (d, *J* = 5 Hz, 2Hβ); 8.64 (d, *J* = 4.5 Hz, 2Hβ); 8.63 (d, *J* = 7 Hz, 2H<sub>3</sub>); 8.62 (d, *J* = 5 Hz, 2Hβ); 8.58 (d, *J* = 4.5 Hz, 2Hβ); 8.52 (d, *J* = 8 Hz, 2H<sub>3</sub>); 8.47 (s, 2NH); 7.96 (d, *J* = 7 Hz, 2H<sub>6</sub>); 7.88 (d, *J* = 7 Hz, 2H<sub>3</sub>);

(6) Boitrel, B.; Lecas-Nawrocka, A.; Rose, E. *Tetrahedron Lett.* **1991**, 32, 2129–2132.

(7) Boitrel, B.; Lecas, A.; Renko, Z.; Rose, E. *New J. Chem.* **1989**, 13, 73–99.

\* Corresponding author. E-mail: bboitrel@satie.u-bourgogne.fr.

<sup>†</sup> Present address: Laboratoire de Synthèse Organique et Organométallique, UMR CNRS 7611, Tour 44, 4 Place Jussieu, 75230 Paris Cedex 05, France.

- (1) (a) Collman, J. P.; Brauman, J. I.; Iverson, B. L.; Sessler, J. L.; Morris, R. M.; Gibson, Q. H. *J. Am. Chem. Soc.* **1983**, 105, 3052–3064. (b) Springer, B. A.; Egeberg, K. D.; Sligar, S. G.; Rohlfis, R. J.; Mathews, A. J.; Olson, J. S. *J. Biol. Chem.* **1989**, 264, 3057–3060.
- (2) Collman, J. P.; Brauman, J. I.; Halbert, T. R.; Suslick, K. S. *Proc. Natl. Acad. Sci. U.S.A.* **1976**, 73, 3333–3337.
- (3) (a) Busch, D. H.; Zimmer, L. L.; Grzybowski, J. J.; Olszanski, D. J.; Jackels, S. C.; Callahan, R. C.; Christoph, G. G. *Proc. Natl. Acad. Sci. U.S.A.* **1981**, 78, 5919–5923. (b) Battersby, A. B.; Hamilton, A. D. *J. Chem. Soc., Chem. Commun.* **1980**, 117–119. (c) Collman, J. P.; Brauman, J. I.; Iverson, B. L.; Sessler, J. L.; Morris, R. M.; Gibson, Q. H. *J. Am. Chem. Soc.* **1983**, 105, 3052–3064. (d) Traylor, T. G.; Tsuchiya, S.; Campbell, D.; Mitchell, M.; Stynes, D.; Koga, N. *J. Am. Chem. Soc.* **1985**, 107, 604–614. (e) Momenteau, M.; Loock, B.; Tétreau, C.; Lavalette, D.; Croisy, A.; Schaeffer, C.; Huel, C.; Lhoste, J. M. *J. Chem. Soc., Perkin Trans. 2* **1987**, 249–257. (f) Hancock, R. D.; Weaving, J. S.; Marques, H. M. *J. Chem. Soc., Chem. Commun.* **1989**, 1176–1178. (g) Uemori, Y.; Kyuno, E. *Inorg. Chem.* **1989**, 28, 1690–1694. (h) Momenteau, M.; Reed, C. A. *Chem. Rev.* **1994**, 94, 659–698 and references therein. (i) Momenteau, M. In *Supramolecular Control of Structure and Reactivity*; Hamilton, A. D., Ed.; (1996) John Wiley and Sons Ltd.: Chichester, 1996. (j) Jaquinod, L.; Prevot, L.; Fischer, J.; Weiss, R. *Inorg. Chem.* **1998**, 37, 1142–1149. (k) Lim, M.; Jackson, T. A.; Anfirud, P. A. *J. Biol. Inorg. Chem.* **1997**, 2, 531–536.
- (4) (a) Ricard, L.; Weiss, R.; Momenteau, M. *J. Chem. Soc., Chem. Commun.* **1986**, 818–820. (b) Kim, K.; Fettinger, J.; Sessler, J. L.; Cyr, M.; Hugdahl, J.; Collman, J. P.; Ibers, J. A. *J. Am. Chem. Soc.* **1989**, 111, 403–405. (c) Kim, K.; Ibers, J. A. *J. Am. Chem. Soc.* **1991**, 113, 6077–6081. (d) Slebodnick, C.; Fettinger, J. C.; Peterson, H. B.; Ibers, J. A. *J. Am. Chem. Soc.* **1996**, 118, 3216–3224. (e) Slebodnick, C.; Ibers, J. A. *J. Biol. Inorg. Chem.* **1997**, 2, 521–525 and references therein.
- (5) Rose, E.; Boitrel, B.; Quelquejeu, M.; Kossanyi, A. *Tetrahedron Lett.* **1993**, 34, 7267–7270.

**Table 1.** Crystal Data and Structure Refinement for ArPyNi (**6**)

compound	ArPyNi ( <b>6</b> )
empirical formula	C <sub>71</sub> H <sub>55</sub> N <sub>13</sub> NiO <sub>8</sub> ·8H <sub>2</sub> O
M	1421.14
T; K	293(2)
cryst syst	monoclinic
space group	<i>P</i> 2 <sub>1</sub>
<i>a</i> ; Å	12.933(2)
<i>b</i> ; Å	17.598(3)
<i>c</i> ; Å	16.996(3)
β; deg	107.69(1)
<i>V</i> ; Å <sup>3</sup>	3685.1(11)
<i>Z</i>	2
F(000)	1488
<i>D</i> <sub>calc</sub> ; g/cm <sup>3</sup>	1.281
λ; Å	0.71073
μ; mm <sup>-1</sup>	0.34
crystal size; mm <sup>3</sup>	0.5 × 0.3 × 0.3
sin(θ)/λ max; Å <sup>-1</sup>	0.62
index ranges	<i>h</i> : -15; 15 <i>k</i> : -21; 2 <i>l</i> : 0; 20
decay	no decay
absorption correction	none
RC = reflens colled	8713
IRC = indep RC	8428 [R(int) = 0.0261]
IRCGT = IRC and [ <i>I</i> > 2σ( <i>I</i> )	7126
refinement method	full-matrix least-squares on <i>F</i> <sup>2</sup>
data/restraints/params	8428/1/885
R for IRCGT	R1 <sup>a</sup> = 0.057, wR2 <sup>b</sup> = 0.157
R for IRC	R1 <sup>a</sup> = 0.076, wR2 <sup>b</sup> = 0.171
goodness-of-fit <sup>c</sup>	1.112
absolute structure parameter	0.01(2)
largest diff peak and hole; e Å <sup>-3</sup>	1.016 and -0.376

<sup>a</sup> R1 = Σ(|*F*<sub>o</sub> - *F*<sub>c</sub>|)/Σ|*F*<sub>o</sub>|. <sup>b</sup> wR2 = [Σw(*F*<sub>o</sub><sup>2</sup> - *F*<sub>c</sub><sup>2</sup>)<sup>2</sup>/Σ[w(*F*<sub>o</sub><sup>2</sup>)<sup>2</sup>]<sup>1/2</sup>, where *w* = 1/[σ<sup>2</sup>(*F*<sub>o</sub><sup>2</sup>) + (0.131*P*)<sup>2</sup>], where *P* = (Max(*F*<sub>o</sub><sup>2</sup>, 0) + 2*F*<sub>c</sub><sup>2</sup>)/3. <sup>c</sup> Goodness of fit = [Σw(*F*<sub>o</sub><sup>2</sup> - *F*<sub>c</sub><sup>2</sup>)<sup>2</sup>/(*N*<sub>o</sub> - *N*<sub>r</sub>)]<sup>1/2</sup>.

7.87 (t, *J* = 7 Hz, 2H<sub>4</sub>); 7.83 (d, *J* = 7 Hz, 2H<sub>4</sub>); 7.67 (s, 2NH'); 7.56 (t, *J* = 7 Hz, 2H<sub>5</sub>); 7.47 (t, *J* = 7 Hz, 2H<sub>5</sub>); 6.50 (d, *J* = 2 Hz, 2H<sub>o</sub>); 5.20 (t, *J* = 2 Hz, 1Hp); 4.83 (s, 4Ht); 4.64 (d, *J* = 7 Hz, 2NHaa); 4.35 (quint, *J* = 7 Hz, 2CHMe); 4.20 (quint, *J* = 7 Hz, 2CH'Me); 3.99 (d, *J* = 7 Hz, 2NHaa'); 1.25 (d, *J* = 7 Hz, 6Me); 1.15 (d, *J* = 7 Hz, 6Me').

#### X-ray Experiments. Crystal Structure of Complex ArPyNi (**6**).

A dark red crystal of **6** (0.4 × 0.3 × 0.3 mm<sup>3</sup>) was mounted on a CAD4 Enraf-Nonius diffractometer. The data were collected at room temperature with graphite-monochromatized Mo -Kα radiation. A total of 8713 intensities, collected up to sin θ/λ = 0.62 Å<sup>-1</sup>, were reduced with the XCAD4PC data reduction program.<sup>8</sup> No decay was observed. The structure was solved via a Patterson search program and refined (space group *P*2<sub>1</sub>) with full-matrix least-squares methods<sup>9</sup> based on |*F*<sup>2</sup>| using all 8428 independent reflections. Experimental details are reported in Table 1. All non-hydrogen atoms were refined with anisotropic thermal parameters. Hydrogen atoms of the complex were included in their calculated positions and refined with a riding model. The absolute configuration of the four chiral centers belonging to the alanine residuals was set to (*S*). Three oxygen atoms of water molecules were located in hydrogen-bonding position to three amide nitrogen atoms and anisotropically refined. At the end of the refinement, the residual indices were somewhat high and the Fourier difference map showed large regions with diffuse residual electron densities. In accordance with the chemical analysis, these residual densities were modeled by the introduction of five more isotropic oxygen atoms of water molecules that form a hydrogen-bonding net around the porphyrin complex. The final difference Fourier map was not sufficiently clear to locate additional molecules. Final agreement indices are *R*<sub>w</sub>(*F*<sup>2</sup>) = 0.171 and *R*(*F*) = 0.076 for all data and 885

parameters, *R*(*F*) = 0.057 for 7126 data with *I* > 2σ(*I*), GOF = 1.112 and Δρ = 1.016 (2.80 Å from O2) and -0.378 e Å<sup>-3</sup>.

## Results and Discussion

The asymmetric unit contains the porphyrin molecule itself and eight interstitial water molecules arranged in a hydrogen bond net around the complex. The porphyrin molecule **6**, represented in Figure 1, consists of a TAPP-based macrocycle with two straps anchored through an amide linkage to the ortho position of two opposite phenyl groups of 5,10,15,20-tetrakis-(*o*-aminophenyl)nickel porphyrin. The distal strap is an *N,N'*-((1,4-dicarbonylphenyl)-*L*-alanyl) residue while the proximal one, located on the opposite face of the macrocycle, is an *N,N'*-((1,4-dicarbonylpyridyl)-*L*-alanyl) group. As expected for such a cross-*trans*-linked structure (αβββ)<sup>10</sup> and even though the β pyrrolic positions are not substituted,<sup>11</sup> the macrocycle exhibits a ruffled conformation: the average Cm deviation is 0.52 Å with respect to the 24-atom least-squares plane and the average dihedral angle of two opposite pyrrole planes is 32.9°. It is noteworthy that rather than pulling the meso carbon atoms out of the porphyrin plane, the straps push on these atoms. The four nitrogen atoms and the Ni atom lie in the 24-atoms plane and the average Ni-N distance is 1.921(4) Å. The phenyl cap, parallel to the 4N plane, stands precisely in the apical position of the Ni atom and a very short distance of 3.40 Å is observed between the Ni atom and the center of the phenyl group. The pyridyl ring of the proximal strap is not parallel to the 4N plane; the dihedral angle between the two planes is 13.6°. Due to the 1,3 linkage of the pyridyl group, the latter does not lie in an apical position: the shortest distance between the Ni atom and the pyridyl group is observed for Ni-C<sub>para</sub> with a value of 3.40 Å.

From the <sup>1</sup>H NMR data of ArPyNi (**6**), we can confirm that the nitrogen base is not bound to the metal. This is revealed by the relative chemical shifts of the pyridine ring protons: 6.5 and 5.2 ppm, respectively, for the ortho and para protons (see Figure 1 for naming the different key protons). Indeed, for complexes in which the pyridine is coordinated to the metal, two different cases are to be distinguished: the five-coordinate one for which the ortho and para protons would be respectively shifted around 135 and 20 ppm<sup>12</sup> and the six-coordinate one—*e.g.*, ArPyFeCO (**2**)—for which the same signals appear at 1.68 and 6.74 ppm.<sup>6</sup> In fact, the preference for a four-coordinate geometry is not due to the metal itself but rather to the structure of the porphyrin as shown in the cases of ArPyFe(II) (**4**) (Figure 2) and ArPyZn(II) (**5**) (5.5 and 4.9 ppm, respectively, for the ortho and para protons of the pyridine ring). Indeed, while nickel(II) prefers a square-planar geometry, zinc(II) prefers to be five-coordinate, often by coordinating a water or methanol molecule,<sup>13</sup> and iron(II) prefers five- or six-coordination depending on the ligands available. It is clear that in the case of the discussed structure, whatever the metal, the complex remains four-coordinate and the nitrogen atom of the intramolecular base is turned toward the outside of the cage as in the free-base (6.50 and 5.20 ppm for the ortho and para pyridinic protons of **6**).

The X-ray structure of the nickel complex **6** (Figure 3) can help us to understand the previously reported properties of the

(8) Harms, K. (harms@mail.uni-marburg.de)

(9) Sheldrick, G. M. *SHELXL: Program for Crystal Structure Refinement*; Sheldrick, G. M., Ed.; University of Göttingen: Göttingen, Federal Republic of Germany, 1997.

(10) Schappacher, M.; Fischer, J.; Weiss, R. *Inorg. Chem.* **1989**, *28*, 389.

(11) Sparks, L. D.; Medforth, C. J.; Park, M. S.; Chamberlain, J. R.; Ondrias, M. R.; Senge, M. O.; Smith, K. M.; Shelnut, J. A. *J. Am. Chem. Soc.* **1993**, *115*, 581–592.

(12) Momenteau, M. *Pure Appl. Chem.* **1986**, *58*, 1493–1502.

(13) Collman, J. P.; Herrmann, P. C.; Fu, L.; Eberspacher, T. A.; Eubanks, M.; Boitrel, B.; Hayoz, P.; Zhang, X.; Brauman, J. I.; Day, V. W. *J. Am. Chem. Soc.* **1997**, *119*, 3481–3489.

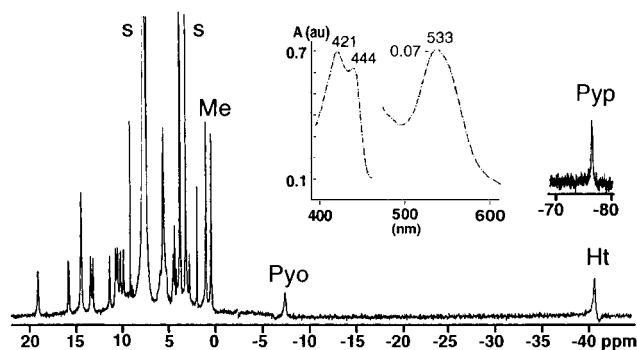


**Figure 2.**  $^1\text{H}$  NMR spectrum of porphyrin ArPyFe(II) (**4**) in  $\text{CDCl}_3$  at 200 MHz, adapted from ref 16b. For detailed chemical shifts, see ref 16a. The inset shows the UV-vis spectrum (MeOH) of the same molecule.

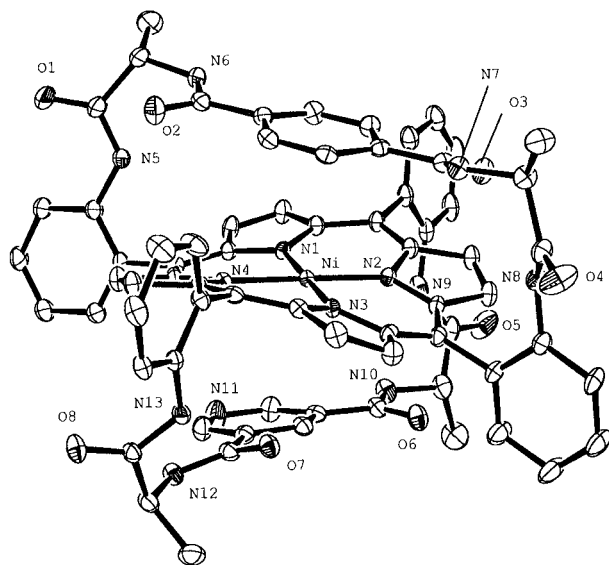


**Figure 3.** ORTEP view of the solid-state structure for ArPyNi (**6**) (for clarity, ellipsoids are set to the 30% probability level and the solvent molecules are not represented).

iron(II) complex **4**, e.g., its low affinity for CO ( $p_{1/2} = 5.5$  Torr).<sup>14</sup> Furthermore,  $^1\text{H}$  NMR and UV-vis spectra of ArPyFe(II) (**4**) (Figure 2) clearly show that the metal remains four-coordinate<sup>15</sup> without any interaction of the built-in nitrogen ligand,<sup>16</sup> and the distance between the porphyrin and the distal strap is, to our knowledge, the shortest ever reported (3.4 Å)

(14) Tétreau, C.; Boitrel, B.; Rose, E.; Lavalette, D. *J. Chem. Soc., Chem Commun.* **1989**, 1805–1806.

(15) It is important to remind that if the distal strap bears two more carbon atoms, the iron(II) complex analogue of **4** is, as expected, a five-coordinate ( $S = 2$ ) complex, leading to  $\text{ArC}_2\text{PyFeCO}$  (**1**) with a  $P_{1/2}(\text{CO}) = 0.2$  Torr after exposure to atmospheric pressure of CO.

for this type of structure. It is known that in the absence of a fifth ligand, the equilibrium constant for CO binding is reduced and reversible oxygenation does not occur due to extremely rapid rates of autoxidation. We have here to emphasize the fact that the binding of oxygen on compound **4** always led to the paramagnetic hydroxo iron(III) porphyrin and never to the diamagnetic oxygenated compound. This unexpected behavior is consistent with the structure of ArPyNi (**6**) because, in the case of the iron(II) complex, both CO and  $\text{O}_2$  bind to a four-coordinate compound but whereas the oxygen complex leads to the hydroxo oxidized species,<sup>17</sup> CO is very likely able to induce the pyridyl coordination owing to its trans effect.<sup>18</sup> In terms of the distortion of the porphyrin ring itself, we proposed a doming of the porphyrin core on the basis of unusual downfield chemical shifts for the  $\beta$ -pyrrolic protons:<sup>16a</sup> Figure 3 shows this severe lack of planarity. If the same distortion occurred in ArPyFe(II) (**4**), this could explain why, in terms of steric hindrance, the proximal base does not rotate to coordinate the metal atom. The lack of coordination of the intramolecular ligand is probably due to the structure and length of the distal strap but not of the proximal one, otherwise the complex  $\text{ArC}_2\text{-PyFe(II)-1}$  before CO coordination—would not be five-coordinate. In fact, the X-ray structure of **6** shows an orientation of the nitrogen base which is consistent with previous predictions from solution  $^1\text{H}$  NMR studies.

### Conclusion

The structure reported herein with a redox-inactive metal such as nickel points out several elements of the porphyrin that may influence the affinity (and presumably the geometry) of the CO binding to iron(II) porphyrins. Among them, we emphasize the distortion of the porphyrin ring induced by the distal strap itself. Indeed, the four peptidic bonds in each strap—because of their rigidity—are likely responsible for both the unexpected four-coordinate geometry by maintaining the pyridine at a very short distance from the porphyrin and the lack of porphyrin planarity. These different characteristics could influence the binding of carbon monoxide in the iron complex ArPyFeCO (**2**). Work is still in progress to obtain single crystals of the carbonyl adduct with the built-in nitrogen base coordinated to the iron(II).

**Supporting Information Available:** Full details of the crystal structure analysis of **6**, in CIF format, are available on the Internet only. Access information is given on any current masthead page.

IC980499M

(16) (a) Boitrel, B.; Lecas, A.; Rose, E. *Tetrahedron Lett.* **1988**, 29, 5653–5656. (b) Boitrel, B. Ph.D. Dissertation, Université Pierre et Marie Curie, Paris, 1989.

(17) Because of its very rigid “peptide-like” straps, this type of model cannot undergo autoxidation via the  $\mu$ -peroxo mechanism but rather by the incompletely understood superoxide pathway (see reference 3h for details).

(18) Buchler, J. W.; Kokisch, W.; Smith, P. D. *Struct. Bonding* **1978**, 34, 79–134.